SUPPLEMENTAL MATERIALS

METHODS

Isolation of peripheral blood mononuclear cells (PBMCs)

PBMCs were extracted from blood samples as previously described [32]. Briefly, 5 mL blood samples were collected from healthy subjects (n=3) without congenital or acquired heart disease under an approved IRB protocol at Nationwide Children's Hospital (NCH). Blood was transferred to a cell separation tube (BD Vacutainer CPT tube, BD Biosciences) and centrifuged at 1,500g for 30 min at room temperature (RT). PBMCs were concentrated in a whitish layer just under the plasma layer and transferred to a 15-mL conical tube. Cells were washed with 10 mL DPBS (Ca^{2+}/Mg^{2+} free) by spinning at 300*g* for 15 min at RT. Cell pellets were resuspended in freezing media (Knockout Serum Replacement plus 10% DMSO) and stored in liquid nitrogen (N2) until iPSC reprogramming.

Human iPSC reprogramming

Frozen PBMCs were thawed and seeded in PBMC culture media containing 1x StemPro-34 SFM supplemented with SCF, FLT3, IL3, IL6 and EPO (Thermo Fisher Scientific). PBMCs were incubated in 5% CO_2 at 37 °C for 7 days with replacement of half of old media with new media. PBMCs were transfected with CytoTune-iPSC 2.0 Sendai Reprogramming Kit (Thermo Fisher Scientific) containing four Yamanaka transcription factors according to the manufacturer's instructions. Emerging iPSC clones were individually picked and transferred to a Matrigel-coated 24-well plate. Stable iPSC lines were established after at least 5 passages. All human iPSC lines were derived and maintained in chemically defined Essential 8 Medium (Thermo Fisher Scientific) in Matrigel-coated plates and passaged using 0.5 mM EDTA for dissociation. Dissociated iPSCs were replated in E8 medium plus 5 μM ROCK inhibitor Y-27632 (Selleckchem) overnight and refreshed with the complete E8 medium thereafter.

CRISPR/Cas9 genome editing in human iPSCs

For precise genome editing, guide RNAs were designed using an online tool CRISPick created by the Broad Institute (https://portals.broadinstitute.org/gppx/crispick/public). To target *NOTCH1* gene,

two sets of guide RNAs were used to generate double cuts in the genome. Guide RNAs were inserted into an expression CRISPR vector pSpCas9(BB)-2A-GFP (PX458, Addgene plasmid #48138). Human iPSCs were transfected with two PX458 vectors containing guide RNAs targeting exon 1 and exon 2 of *NOTCH1* gene, respectively. Lipofectamine LTX Reagent with PLUS Reagent (Thermo Fisher Scientific) was used for transfection of iPSCs. Flow cytometry was performed two days after transection and the GFP^{high} cell population was selected. These GFP^{high} iPSCs were seeded at low density (100 cells per well of a 6-well plate) to obtain single-cell iPSC clones. Individual iPSC clones were picked and seeded into one well of a 24-well plate. Genomic DNA was extracted from these iPSC clones using the QuickExtract DNA Extraction Solution (Lucigen). Separate PCRs using both outside primers and inside primers were performed. Sanger sequencing were carried out to confirm the genotypes of N1KO iPSC clones. Prospective off-target sites were screened to eliminate off-target editing in these iPSC clones. CRISPRoff package was employed to evaluate the specificity of gRNAs and bulk RNA-seq data was used to assess the off-target effects [71]. The expression of predicted off-target target genes showed negligible change in N1KO iPSC lines.

Cardiomyocyte differentiation

Cardiac differentiation was performed according to a protocol we previously published [26, 32]. Briefly, iPSCs were cultured on Matrigel to reach over 90% confluency when differentiation media was introduced. Cells were incubated with 6 μM CHIR99021 (Selleckchem) in basal differentiation media (RPMI1640 medium plus B27 minus insulin supplement) for 2 days, followed by incubating with basal differentiation media for 1 day. Cells were then treated with 5 μM IWR-1 (Sigma) in basal differentiation media for 2 days, followed by incubating with basal differentiation media for another 2 days. On day 7, cardiac maintenance media (RPMI1640 medium plus B27 supplement) was introduced. Beating clusters were observed at days 8-12 of differentiation. To remove non-cardiomyocytes, glucose was deprived from the culture by incubating with cardiac purification media (RPMI1640 no glucose medium plus B27 supplement) for 4 days. Regular cardiac maintenance media was introduced after glucose deprivation. For passaging iPSC-CMs, TrypLE Select Enzyme 10x (Thermo Fisher Scientific) was used to dissociate

them into single cells. After centrifuging at 300*g* for 5 min, supernatants were removed. Cells were resuspended and replated into a Matrigel-coated 6-well plate using cardiac replating media (cardiac maintenance media plus 10% KSR).

Vascular endothelial differentiation

Vascular endothelial differentiation was performed as previously described [72]. When iPSCs reached 90-95% confluency, endothelial differentiation was initiated by adding the basal differentiation media plus 6 μM CHIR99021 for 2 days. Cells were then incubated with 3 μM CHIR99021 in the basal differentiation media for another 2 days. On Day 4 (D4), endothelial differentiation media [EGM-2 medium plus 50 ng/mL VEGF (PeproTech), 20 ng/mL bFGF (PeproTech), and 10 μM TGF-β inhibitor SB431542 (Selleckchem)] was introduced and media was changed every other day. At D10 of differentiation, cells were sorted by magnetic-activated cell sorting using human CD31 microbeads (Miltenyi Biotec). The sorted CD31+ iPSC-ECs were seeded in 0.2% gelatin-coated plates and maintained in EGM-2 medium (Lonza) supplemented with 50 ng/mL of recombinant human VEGF.

Real time qPCR

Total RNA extraction was performed using the Direct-zol RNA Miniprep Kits (Zymo Research) accordingly to the manufacturer's protocol. Reverse transcription was carried out using the iScript Reverse Transcription Supermix for RT-qPCR (Bio-Rad). The diluted cDNA was added for real time PCR using Taqman Gene expression Assays (**Table S3**) and Taqman Fast Advanced Master Mix (Thermo Fisher Scientific) in the StepOnePlus Real-time PCR system. The PCR program was the following: hold at 50 °C for 2 minutes, hold at 95 °C for 20 seconds, denature at 95 °C for 1 second, and anneal/extend at 60 °C for 20 seconds for 40 cycles. C_T values were measured and transformed to relative gene expression levels by the $2\text{-}\Delta\Delta C_T$ method.

MitoTracker assay

Human iPSC-CMs were incubated with 40 nM MitoTracker Green (Thermo Fisher Scientific) for 15 min at 37°C followed by nuclear staining with Hoechst 33342. Fluorescence images were taken using a Keyence microscope and processed using ImageJ. Fluorescence intensity of single cells was quantified and subtracted from the background. Fifty individual cells from WT or N1KO were measured for each experiment, which was repeated at least 3 times.

Immunofluorescence

Cultured cells were washed with DPBS twice and fixed using 4% paraformaldehyde (Electron Microscopy Sciences) for 15 min at RT. Cells were then washed with PBS and incubated with 0.1% Triton X-100 (Sigma) for 10 min at RT. Cells were washed twice with PBS and subsequently blocked with 0.2% BSA (Sigma) in PBS for 1h at RT. After blocking, cells were incubated with a primary antibody diluted in the blocking solution at 4°C overnight. Cells were washed with blocking solution for 3 times and then incubated with a secondary antibody for 1h at RT. Cells were washed with PBS for 3 times. Nuclei were counterstained with DAPI for 10 min at RT. Following final wash, cells were mounted using SlowFade Gold Antifade Mountant (Thermo Fisher Scientific) on a microscope slide. Immunofluorescent slides were visualized and captured by an inverted fluorescence microscope (Keyence) or a confocal microscope (Zeiss). Primary antibodies used in this study are: alpha-actinin (Sigma, A7811), cardiac troponin T (Abcam, ab45932), NOTCH1 (Cell Signaling Technology, #4147), Ki67 (Abcam, ab15580), Cyclin D1 (Cell Signaling Technology, #55506), MYL2 (Abcam, ab79935), COUP-TFII (R&D Systems, PP-H7147-00), NKX2-5 (Thermo Fisher Scientific, PA5-49431), ISL1 (Thermo Fisher Scientific, MA5-15515), WT1 (Proteintech, 12609-1-AP), TBX18 (R&D Systems, mab63371), TBXT (R&D Systems, AF2085), TBX6 (Thermo Fisher Scientific, PA5-35102), Phospho-Rb (Cell Signaling Technology, #8516), Alexa Fluor 488 mouse anti-human CD31 (BD Biosciences, 558068), and Alexa Fluor 647 mouse anti-human CD144 (BD Biosciences, 561567), Rabbit IgG Isotype Control (Abcam, ab172730), Mouse IgG Isotype Control (Abcam, ab37355), Goat IgG Isotype Control (Abcam, ab37373). Mouse/rabbit/goat IgG isotype controls

were used for validating the specificity of primary antibodies. Samples with secondary antibodies only were used as negative controls for distinguishing positive signals from the background.

DAPT treatment

The γ-secretase inhibitor, DAPT (5 μM in DMSO), was added to the cardiac differentiation media throughout the differentiation. 0.05% DMSO was used as the vehicle control. D30 iPSC-CMs were fixed and subjected to immunofluorescence staining as described above. An antibody against MYL2 was used for identifying ventricular-like cardiomyocytes in the population. Ratios of TNNT2+ MYL2+ cells versus TNNT2+ cells indicate the percentage of ventricular-like cardiomyocytes.

Flow cytometry

Cultured monolayer cells were lifted up using TrypLE Express Enzyme 1X (Thermo Fisher Scientific) and filtered through a cell strainer cap of a FACS tube (BD Biosciences). Cells were then incubated in BD Cytofix/Cytoperm Solution (BD Biosciences) for 20 min for fixation at 4 °C. Cells were washed with 1X BD Perm/Wash buffer (BD Biosciences) once. Subsequently, fixed cells were incubated with primary antibodies diluted in 1X BD Perm/Wash buffer for 30 min on ice. Primary antibodies were removed by spinning at 300xg for 5 min and discarding the supernatant. Cells were washed again using 1X BD Perm/Wash buffer. Cells were then incubated with secondary antibodies diluted in 1X BD Perm/Wash buffer. Secondary antibodies were removed by washing with 1X BD Perm/Wash buffer twice. Cell pellets were resuspended in FACS buffer (PBS plus 1% FBS and 2 mM EDTA) and loaded to a BD FACS Aria II instrument at Nationwide Children's Hospital.

Single-cell RNA-seq

A Chromium Next GEM Single Cell 3' GEM, Library & Gel Bead Kit v3.1(10x Genomics, PN100021) was used for single-cell library preparation. Briefly, cells were dissociated and counted to ensure the preferred cell concentration and viability. Single-cell suspensions were processed and loaded into a Chromium Next GEM Chip G (10x Genomics, PN 200177) to generate single-cell gel bead-in-

emulsions (GEMs) on a 10x Genomics Chromium Controller. cDNA amplifications were performed according to the manufacturer's instructions. Amplified cDNA with individual indexes from a Single Index Plate T Set A (10x Genomics, PN2000240) was used for single-cell library construction. The concentration and size of the constructed libraries were determined using the High Sensitivity D1000 ScreenTape on Agilent 4200 TapeStation. Individual single-cell libraries were pooled and loaded to an Illumina NovaSeq 6000 system for sequencing.

Bulk RNA-seq

For total RNA extraction, cells were lysed by the TRIzol Reagent (Thermo Fisher Scientific). Cell lysate was stored at -80 °C until RNA extraction. Cell lysate was processed for total RNA extraction using the Direct-zol RNA Miniprep Kit (Zymo Research). Total RNA was quantified using a Qubit 4 Fluorometer (Thermo Fisher Scientific). RNA integrity was evaluated by an Agilent 2100 Bioanalyzer (Agilent Technologies). For RNA-seq library construction, mRNA was enriched using oligo(dT) beads and then fragmented randomly. Complementary DNA (cDNA) was synthesized using random hexamers primers. After a series of terminal repair and adaptor ligation, double-stranded cDNA library was completed through size selection and PCR enrichment (Illumina). Qualified cDNA libraries were loaded to Illumina NovaSeq 6000 system for deep sequencing.

Whole-cell patch clamp

Human iPSC-CMs were dissociated into single cells and seeded at a low density on a gelatin-coated coverslip and cultured for a week in cardiac maintenance media. Action potentials, I_{Kr}, I_{to}, I_{Ca}, and I_{Na} currents were all recorded using the whole-cell configuration of the patch clamp technique at 35 °C except I_{Na} currents at room temperature. For recording action potentials, I_{Kr} and I_{to}, cells were bathed with Tyrode's solution composed of NaCl (137 mM), KCl (5.4 mM), $CaCl_2$ (2.0 mM), $MgCl_4$ (3.5 mM), glucose (10 mM), HEPES (10 mM) and pH to 7.35 with NaOH. Patch pipettes were pulled from borosilicate capillary glass with resistance 0.9-1.5 MΩ when filled with electrode solution composed of aspartic acid (120 mM), KCl (20 mM), $MgCl_2$ (2 mM), HEPES (5 mM), NaCl (10 mM), EGTA (5 mM), Na-GTP (0.3

mM), phosphocreatine (14 mM), K-ATP (4 mM), creatine phosphokinase (2 mM) and brought to pH of 7.2. For action potentials, cells were paced in the current clamp mode using a 1.5 - 2 diastolic threshold 5 ms current pulse at 1 Hz. To measure I_{Kr}, currents were elicited from a holding potential of -40 mV with depolarizing voltage pulses from -20 mV to 40 mV for 2 s and I_{Kr} were measured as tail current component upon return to -40 mV. To measure I_{to}, cells were placed in a Tyrode's solution containing nisoldipine (1 μmol/L) to block calcium current and calcium-activated chloride current and TTX (100 μmol/L) to block sodium current. Cells were brought from a holding potential of –70 mV to –25 mV for 25 ms to further inactivate sodium current. I_{to} amplitude was measured as the difference between peak current and steady-state current during a 400 ms voltage step ranging from –30 to +60 mV that immediately followed. When measuring I_{Ca} and I_{Na} microelectrodes were filled with a solution of CsMES (130 mM), TEA Cl (20 mM), $MgCl_2$ (1 mM), HEPES (10 mM), EGTA (10 mM), TRIS GTP (0.3 mM), phosphocreatine (14 mM), Mg ATP (4 mM), creatine phosphokinase (2 mM) and brought to pH of 7.3. I_{Ca} were elicited from a holding potential of -40 mV with depolarizing voltage pulses from -30 mV to 60 mV for 300 ms when cells were placed in the solution containing NaCl (137 mM), CsCl (5.4 mM), $MgCl_2$ (1.8 mM), $CaCl_2$ (2 mM), glucose (10 mM), HEPES (10 mM), pH 7.3. I_{Na} were elicited from a holding potential of -80 mV with depolarizing voltage pulses from -60 mV to 45 mV for 16 ms when cells were placed in the solution containing NaCl (25 mM), N-methyl D-glucamine (120 mM), CsCl (5.4 mM), $MgCl_2$ (1.8 mM), $CaCl_2$ (1.8 mM), glucose (10 mM), HEPES (10 mM) with pH 7.3. nisoldipine (1 μM) was used to block L-type Ca currents. All ionic current density (pA/pF) was calculated from the ratio of current amplitude to cell capacitance. Command and data acquisition were operated with an Axopatch 200B patch clamp amplifier controlled by a computer using a Digidata 1200 acquisition board driven by pCLAMP 7.0 software (Axon Instruments).

Seahorse assay

Cardiomyocyte mitochondrial function was measured using a Seahorse XF Cell Mito Stress Test Kit (Agilent). Cells were seeded (50,000 cells/well) in cardiac maintenance media in Seahorse XF96 Cell Culture Microplates and cultured for a week. Experiments were performed using the Seahorse XF base

medium plus 5 mM glucose, 2 mM L-glutamine, and 1 mM sodium pyruvate. Cells were incubated in the abovementioned media for 1 h before measurement. Oxygen consumption rate was measured sequentially in the presence of 2.5 μM oligomycin (ATPase inhibitor), 5 μM carbonyl cyanide 3-chlorophenylhydrazone (CCCP, uncoupling agent), 2.5 μM rotenone (inhibitor of the mitochondrial complex I), and 2.5 μM antimycin (inhibitor of the mitochondrial respiratory chain). Sequential compound injection was automatically executed by a Seahorse XFe96 Analyzer (Agilent). Basal respiration, ATP production, proton leak, maximal respiration, spare respiratory capacity, and non-mitochondrial respiration were measured. PrestoBlue Cell Viability Reagent (Thermo Fisher Scientific) was used to measure the cell viability for the normalization of oxygen consumption rates.

Cardiac optical mapping

Lentiviral vector infection was performed as previously published [31]. Briefly, D30 human iPSC-CMs were seeded on a Matrigel-coated 35 mm glass bottom dish with 20 mm micro-well (Cellvis). Cells were infected with the lentivirus vector pcDNA3.1/Puro-CAG-ASAP2s (Addgene plasmid #101274) at multiplicity of infection (MOI) of three [73]. Virus was removed 24 h post infection and fresh cardiac maintenance medium was added. Cells were then cultured for 1 week. For optical imaging, cells were incubated in Tyrode's solution at 37 °C. The ASAP2 fluorescence was excited at 488 nm and emission was collected over 510 nm. Line scan images were captured on a confocal microscope (Zeiss LSM 710). Raw image data were processed using a customized MATLAB program.

Western blotting

For protein extraction, cells were washed twice with cold PBS. Cells were then lysed in the RIPA solution plus 1x protease/phosphatase inhibitor and EDTA. Cell lysate was homogenized by sonicating at 45 s for three time, with 45 s intervals in between in a Bioruptor Pico sonication device (Diagenode). Lysate was centrifuged at 14,000xg for 20 min at 4 °C. Supernatants were collected and stored at -80 °C. Protein concentration was measured by a Pierce BCA Protein Assay (Thermo Fisher Scientific). Protein samples were denatured at 95 °C for 3 min and then loaded to a precast SDS-PAGE minigel

(Bio-Rad) in a Mini Gel Tank (Thermo Fisher Scientific) for electrophoresis. After electrophoresis, proteins were transferred to a PVDF membrane in the XCell II Blot Module (Thermo Fisher Scientific) overnight. Membrane was blocked in 5% BSA in TBST buffer (TBS buffer plus 0.1% Tween-20) for 1 h at RT, then incubated with a primary antibody diluted in the blocking buffer at 4 °C overnight with shaking. Membrane was washed 3 times in TBST with shaking before incubating with a secondary antibody for 1 h at RT. Subsequently, membrane was washed 3 times in TBST to remove any residual secondary antibody. For signal visualization, membrane was incubated with the Clarity Western ECL Substrate (Bio-Rad). Chemiluminescent signals were captured using a ChemiDoc Imaging System (Bio-Rad). Primary antibodies for Western blot were: Cleaved Notch1 (Val1744) (D3B8) Rabbit mAb (Cell Signaling Technology, #4147, 1:1000), and GAPDH Loading Control Antibody HRP conjugate (Thermo Fisher Scientific, MA5-15738-HRP, 1:1000). The secondary antibody included Goat anti-rabbit IgG (H+L) HRP conjugate (Bio-Rad, 170-6515, 1:2000).

Bioinformatics analysis

For bulk RNA-seq raw reads, adapter trimming was carried out by Cutadapt (version 3.5) [74]. Quality control analysis of FASTQ files was performed with FASTQC software before and after adapter trimming. The pre-processed reads were aligned to the GRCh38.p13 assembly of the human reference genome using the alignment program HISAT2 (version 2.2.1) [75]. The resulting SAM files were converted to BAM files, then sorted and indexed with SAMtools [76]. Features were identified from the associated GTF file from GENCODE and total counts for each feature were calculated using featureCounts (version 1.6.4) [77]. The DESeq2 [78] R package was used for size factor, dispersion estimation calculation, and data analysis. Significantly differentially expressed genes were identified with a false discovery rate (FDR) less than 0.05 and fold-change (FC) greater than 2. DEG analysis was performed using DESeq2 package and the p-value was adjusted for multiple testing using the Benjamini and Hochberg method. Total number of genes used for test between KO and WT was 43,287. QIAGEN Ingenuity Pathway Analysis (IPA), over representation analysis (ORA), and gene set enrichment analysis (GSEA) were used for pathway and network analysis. All genes were ranked based on adjusted p-values from DESeq2 analysis

and gene set enrichment analysis was performed using “fgsea” package (version 1.22). Multiple testing was performed on the enrichment p-values using the Benjamini and Hochberg method. Gene sets with adjusted p-value less than 0.05 was considered enriched. In total, 1,554 gene sets from Reactome pathway database were used for testing.

Single-cell RNA-seq data were counted by Cell Ranger v4.1.0 using the hg38 reference genome. Data processing and visualizations of the scRNA-seq data were performed using the Seurat R package (v.4.0.4) in R (v.4.1.0) [79]. Our initial dataset included 33,302 cells and 36,601 genes in total. For initial quality control filtering, individual cells with less than 200 genes or more than 25,000 total reads, and genes expressed in less than three cells were removed. Cells that were outside the range of 5x median absolute deviation of total read counts were filtered out. Cells with less than 25% mitochondrial reads in D30 samples and cells with less than 15% mitochondrial reads for all other samples were retained. After quality control, 25,000 single cells and 27,135 genes were included in the downstream analysis. Data were scaled to 10,000 transcripts per cell, and transformed to log-space using Seurat’s LogNormalize function. Highly variable genes in the dataset were computed based on dispersion and mean. Principal component (PC) analysis was performed on the top 2,000 variable genes using Seurat’s RunPCA function. The top 20 PCs were used to build a k-nearest-neighbors cell–cell graph (k = 30). We selected the first 20 principal components (PCs) for clustering and visualization by heuristically checking the Elbow plot of the PCs, which ranks the PCs based on the percentage of variance explained by each one. Clusters were identified using the Louvain graph-clustering algorithm with the resolution set to 0.2. The entire dataset was projected onto the two-dimensional space using uniform manifold approximation and projection (UMAP) dimensionality reduction on the top 20 principal components using Seurat’s RunUMAP function and uwot R package. Cell-type labels were assigned using known marker genes (**Table S4**). Individual cell types were computationally selected for between-group analysis. The differential gene expression analysis was performed using the non-parametric Wilcoxon rank sum test in Seurat’s FindMarkers function. For each comparison, the computed p-values were adjusted to control the false discovery rate (FDR) using the Bonferroni correction for all genes in the dataset. Genes with FDR <0.05 were considered as differentially expressed genes. Over-representation enrichment analysis was

performed to identify gene ontology terms using the Enrichr R package (v.3.0) and GO Biological Process library (v.2018, including 5,103 terms covering 14,433 gene sets) [80]. The p-value from Enrichr was computed using a hypergeometric test that is a binomial proportion test that assumes a binomial distribution and independence for probability of any gene belonging to any set. The q-value from Enrichr is an adjusted p-value using the Benjamini-Hochberg method for correction for multiple hypotheses testing. Enrichr precomputes a background expected rank for each term in each gene set library, which is a lookup table of expected ranks and variances for each term in the library. These expected values are precomputed using hypergeometric test for many random input gene sets for each term in the gene set library. Heatmaps were generated using the ComplexHeatmap on z-score transformed and normalized gene expression values [81].

Pseudotime trajectory analysis using RNA velocity

RNA velocity count matrix for each sample was obtained using the velocyto Python package from the aligned BAM file. The SeuratDisk R package was used to covert the processed R object to the Python object for the scVelo package. After filtering genes with less than 20 spliced and un-spliced counts from the velocity matrix, the moments for velocity estimation were calculated and the splicing kinetic dynamics of genes were inferred by utilizing a built-in function from the scVelo module. Pseudotime was computed based on the velocity graph and the velocity was projected on the diffusion map and visualized as streamlines.

IRIS3 analysis

IRIS3, an integrated web server for cell-type-specific regulon (CTSR) prediction tool [82], was used to computationally identify potential TFs. IRIS3 workflow includes five steps: (i) cell cluster prediction, (ii) functional co-expressed gene module detection, (iii) cell cluster active gene module determination, (iv) de novo motif finding, and (v) TF matching and CTSR determination. Single-cell RNA-seq datasets were analyzed using IRIS3 with the default parameters. Gene regulatory networks were constructed to indicate the predicted TF-gene regulatory relations via Cytoscape.

Human subjects

The protocols involving human subjects in this study were approved by the Institutional Review Board (IRB) at Nationwide Children's Hospital.

Code availability

All code related to the analysis is available at https://github.com/OSU-BMBL/NOTCH1-cardiac-lineage-scRNAseq.

Statistics

Statistical analysis was performed using GraphPad Prism V9.0.2. Kolmogorov-Smirnov test was used for testing normal distribution. Unpaired 2-tailed Student *t*-test was used to compare 2 groups and 1-way ANOVA was used for comparisons among more than 2 groups. A value of $p<0.05$ was considered statistically significantly. Values were shown as a mean±SEM, unless otherwise indicated.

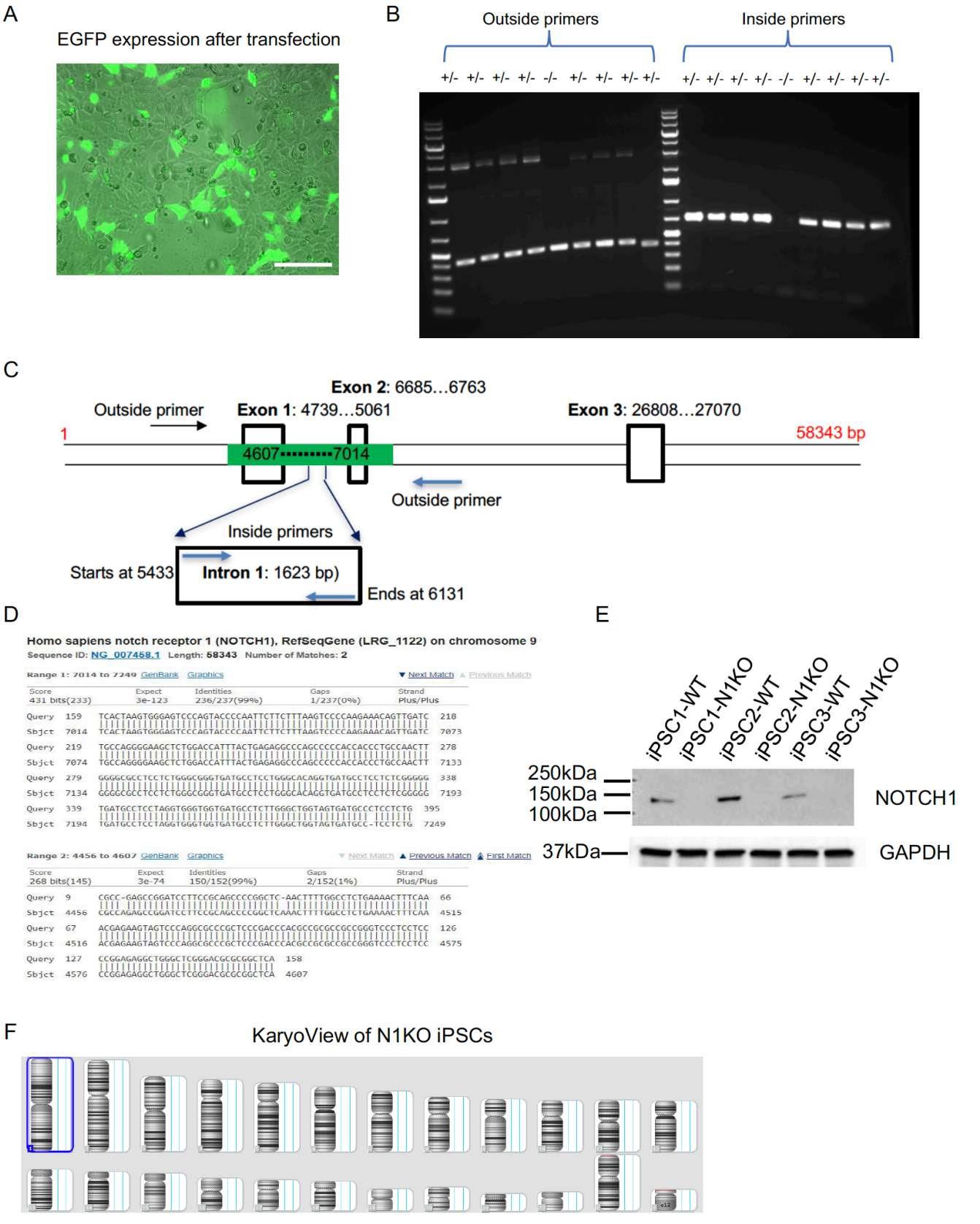

Figure S1. CRISPR/Cas9 genome editing in human iPSCs. (**A**) EGFP expression in human iPSCs 24 h after transfection. Scale bar: 100 μm (**B**) PCR genotyping of single-cell derived iPSC clones using outside and inside primers. (**C**) Genomic locations of outside and inside primers in *NOTCH1* gene locus.

Amplicons using outside primers are flanking the deletion region whereas amplicons using inside primers are within the deletion region. (**D**) NCBI BLAST alignment of Sanger sequencing results with the reference *NOTCH1* sequence. (**E**) Western blot analysis confirms the absence of NOTCH1 protein in all 3 N1KO iPSC lines. (**F**) A representative normal karyotype of N1KO iPSCs revealed by KaryoStat analysis.

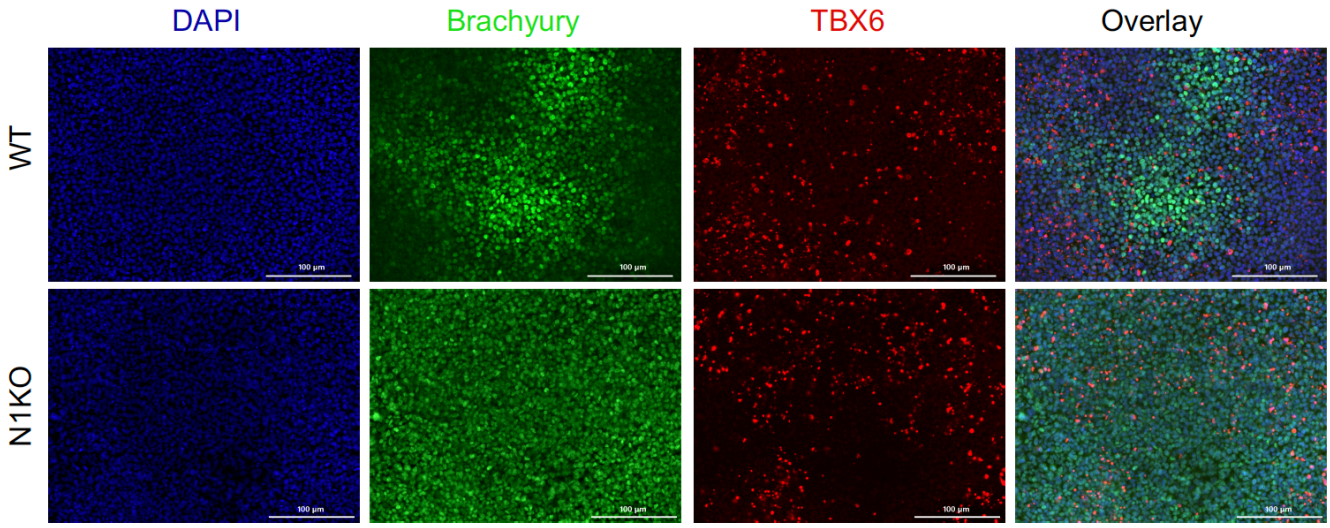

Figure S2. Mesoderm induction of N1KO and WT iPSCs. Mesodermal lineage markers Brachyury (TBXT) and TBX6 were expressed at D2 of cardiac differentiation in both N1KO and WT iPSCs. Scale bars: 100μm.

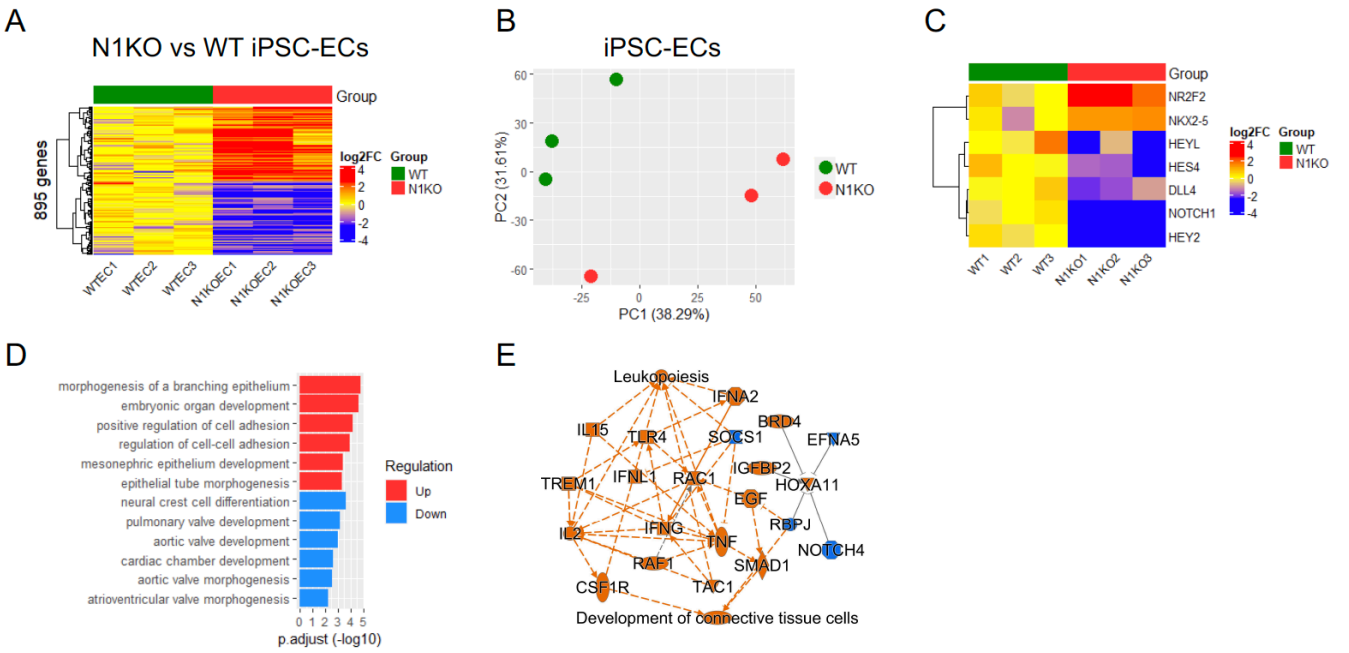

Figure S3. Transcriptional profiling of endothelial cells derived from N1KO and WT iPSCs. (**A**) Heatmap shows 895 differentially expressed genes between WT and N1KO iPSC-ECs (fold change > 2, FDR < 0.05). (**B**) PCA plot indicates the global gene expression variance between WT and N1KO iPSC-ECs. (**C**) Heatmap of upregulated (*NR2F2*, *NKX2-5*) and downregulated (*HEYL*, *HES4*, *DLL4*, *NOTCH1, HEY2*) genes in N1KO compared to WT iPSC-ECs. (**D**) GO biological process pathways that are upregulated (in red) and downregulated (in blue) in N1KO versus WT iPSC-ECs. (**E**) QIAGEN Ingenuity Pathway Analysis indicates a gene interaction network inferred by DEGs between N1KO and WT iPSC-ECs.

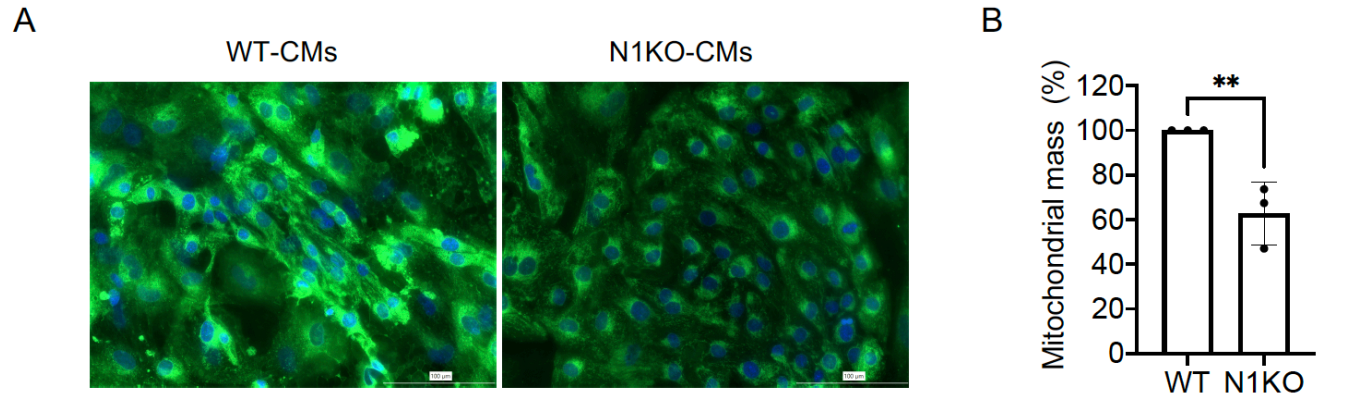

Figure S4. Quantitation of mitochondrial content in N1KO and WT iPSC-CMs. (**A**) Visualization of mitochondria by MitoTracker green in D30 iPSC-CMs. Nuclei are counterstained by DAPI. Scale bars: 100μm. (**B**) Quantitation of mitochondrial mass based on MitoTracker green staining using the ImageJ software (t-test, n=3). Data are presented as mean ± SEM. **p<0.01.

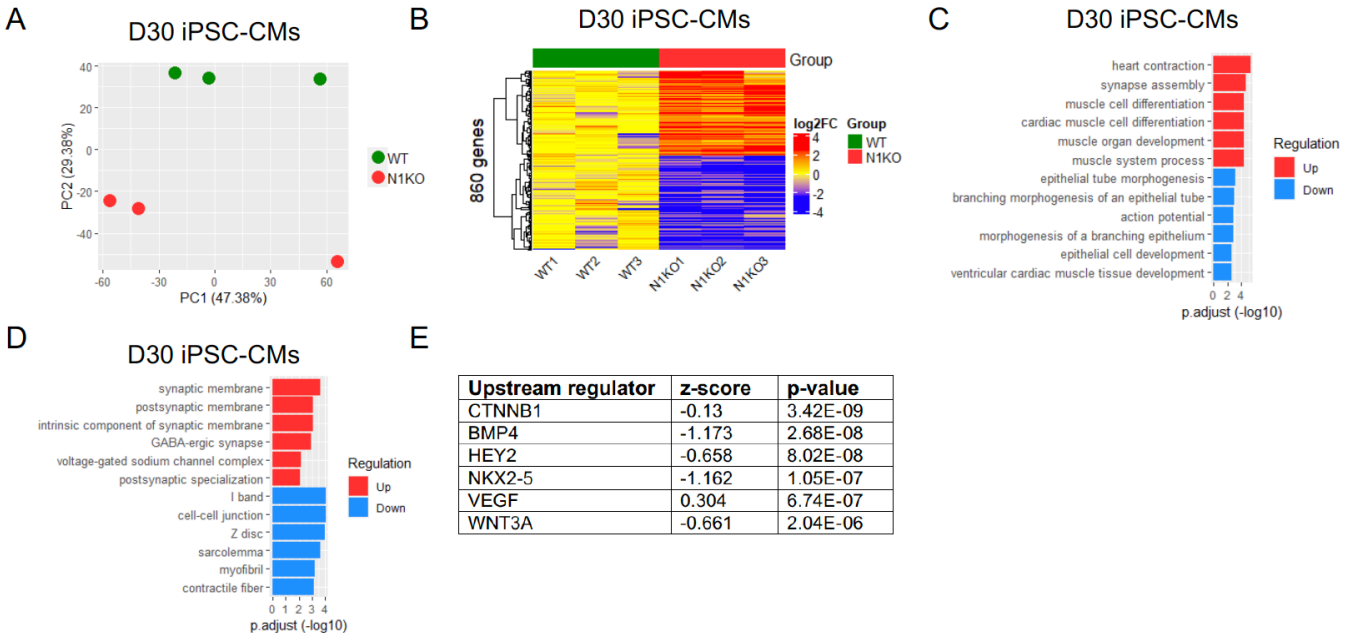

Upstream regulator	z-score	p-value
CTNNB1	-0.13	3.42E-09
BMP4	-1.173	2.68E-08
HEY2	-0.658	8.02E-08
NKX2-5	-1.162	1.05E-07
VEGF	0.304	6.74E-07
WNT3A	-0.661	2.04E-06

Figure S5. Gene expression prolifes of D30 N1KO and WT iPSC-CMs. (**A**) PCA plotting delineates global transcriptional variance between N1KO and WT D30 iPSC-CMs. (**B**) 860 DEGs are identified and shown in the heatmap (fold change >2, FDR<0.05). (**C-D**) GO term enrichment analysis by the domains of biological process (C) and cellular component (D) identifies downregulated and upregulated pathways associated with DEGs between N1KO and WT D30 iPSC-CMs. (**E**) IPA analysis identifies upstream regulators associated with DEGs between N1KO and WT D30 iPSC-CMs.

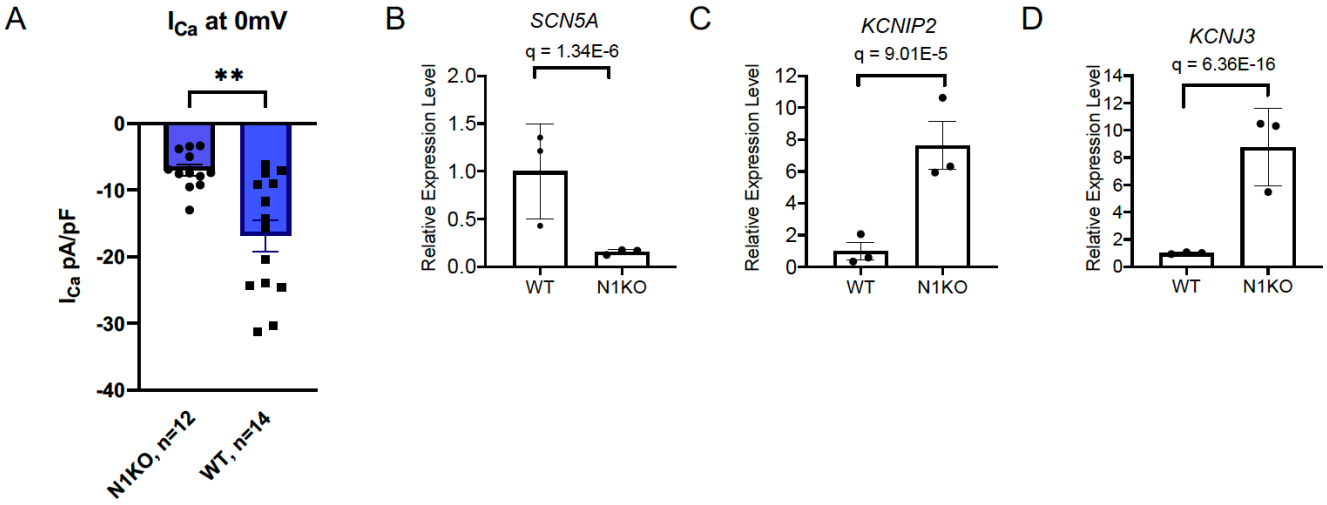

Figure S6. Ion channel activity and gene expression in WT and N1KO D30 iPSC-CMs. (A) Inward Ca^{2+} currents are reduced in N1KO versus WT iPSC-CMs at the depolarizing state (membrane potential = 0 mV). **p<0.01. (**B-D**) Expression levels of ion channel genes *SCN5A*, *KCNIP2*, and *KCNJ3* in WT and N1KO iPSC-CMs measured by RNA-seq (n=3). Data are presented as mean ± SEM. q-values are shown on top of bars.

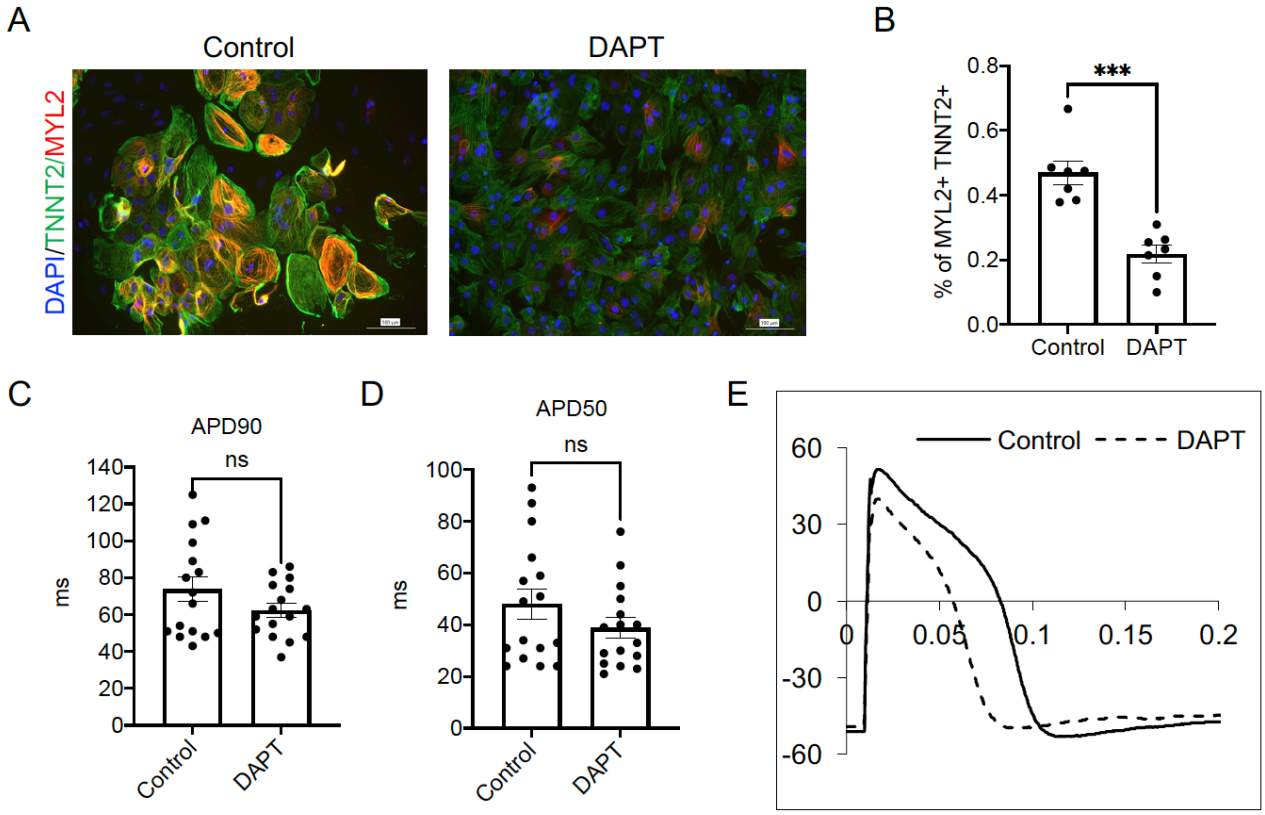

Figure S7. Chemical inhibition of NOTCH signaling by DAPT suppresses ventricular cardiomyocyte differentiation through shortening action potential duration. (**A**) MYL2+ ventricular-like cardiomyocytes are less prevalent in DAPT-treated iPSC-CMs compared to the control. (**B**) Quantitative analysis of the percentage of ventricular-like cardiomyocytes in DAPT and control iPSC-CMs (t-test, n=7, ***p<0.001). (**C-D**) Measurement of APD90 and APD50 in control and DAPT-treated iPSC-CMs by whole-cell patch clamp (t-test, n=16, ns: not significant). (**E**) Shortened action potential duration in DAPT versus control iPSC-CMs revealed by whole-cell patch clamp recording. Scale bars: 100 μm.

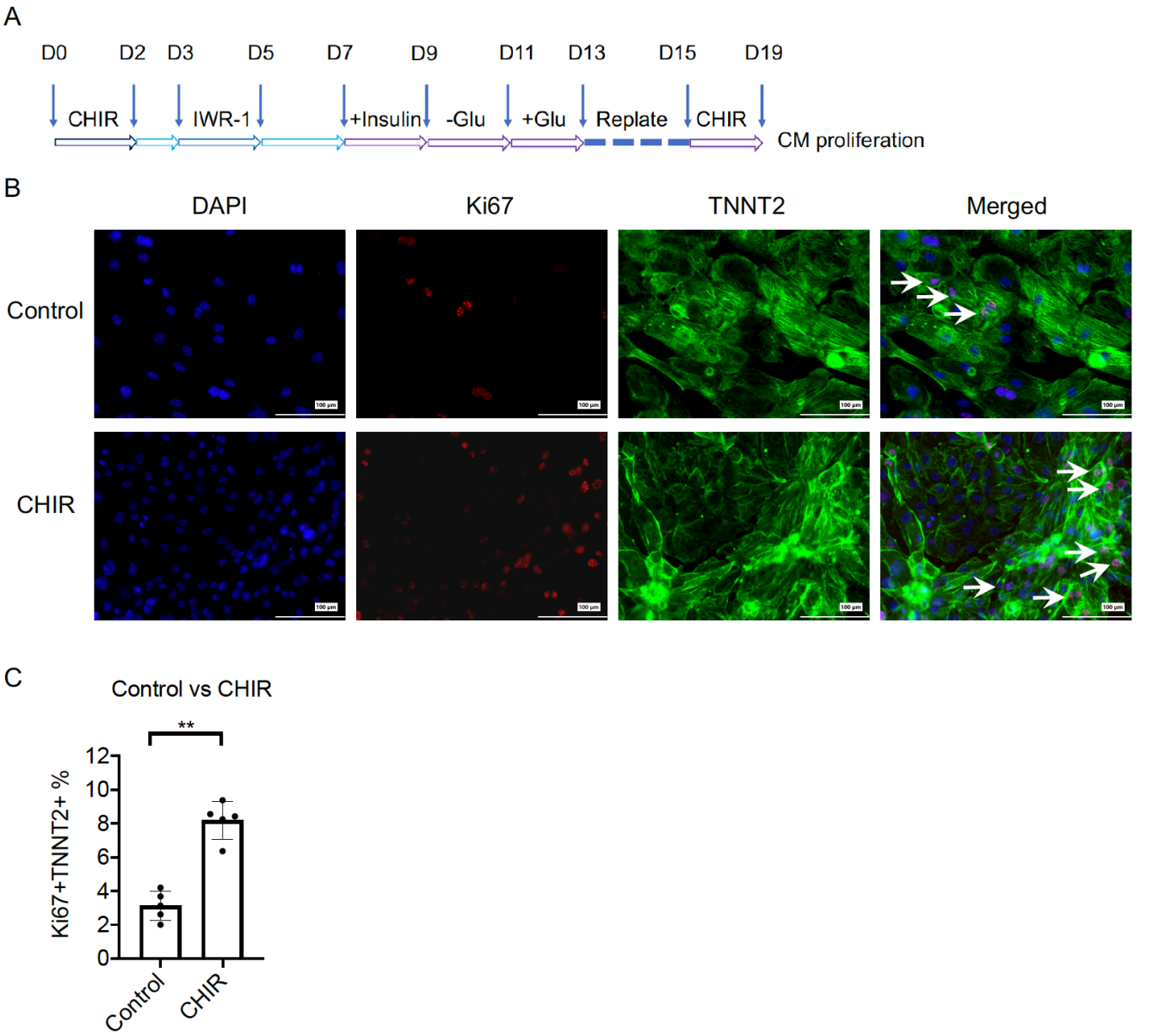

Figure S8. CHIR99021 treatment promotes the proliferation of early iPSC-CMs. (**A**) Graphic overview of an in vitro assay to evaluate the proliferation of early iPSC-CMs. (**B**) Immunocytochemistry staining using antibodies against TNNT2 (green) and cell proliferation marker Ki67 (red). Nuclei are stained with DAPI (blue). Arrows indicate dividing cardiomyocytes. (**C**) Quantitative analysis of the proportion of dividing cardiomyocytes identified by TNNT2+Ki67+ cells. Data are presented as mean ± SEM. **p<0.01, n=5, t-test. Scale bars: 100 μm.

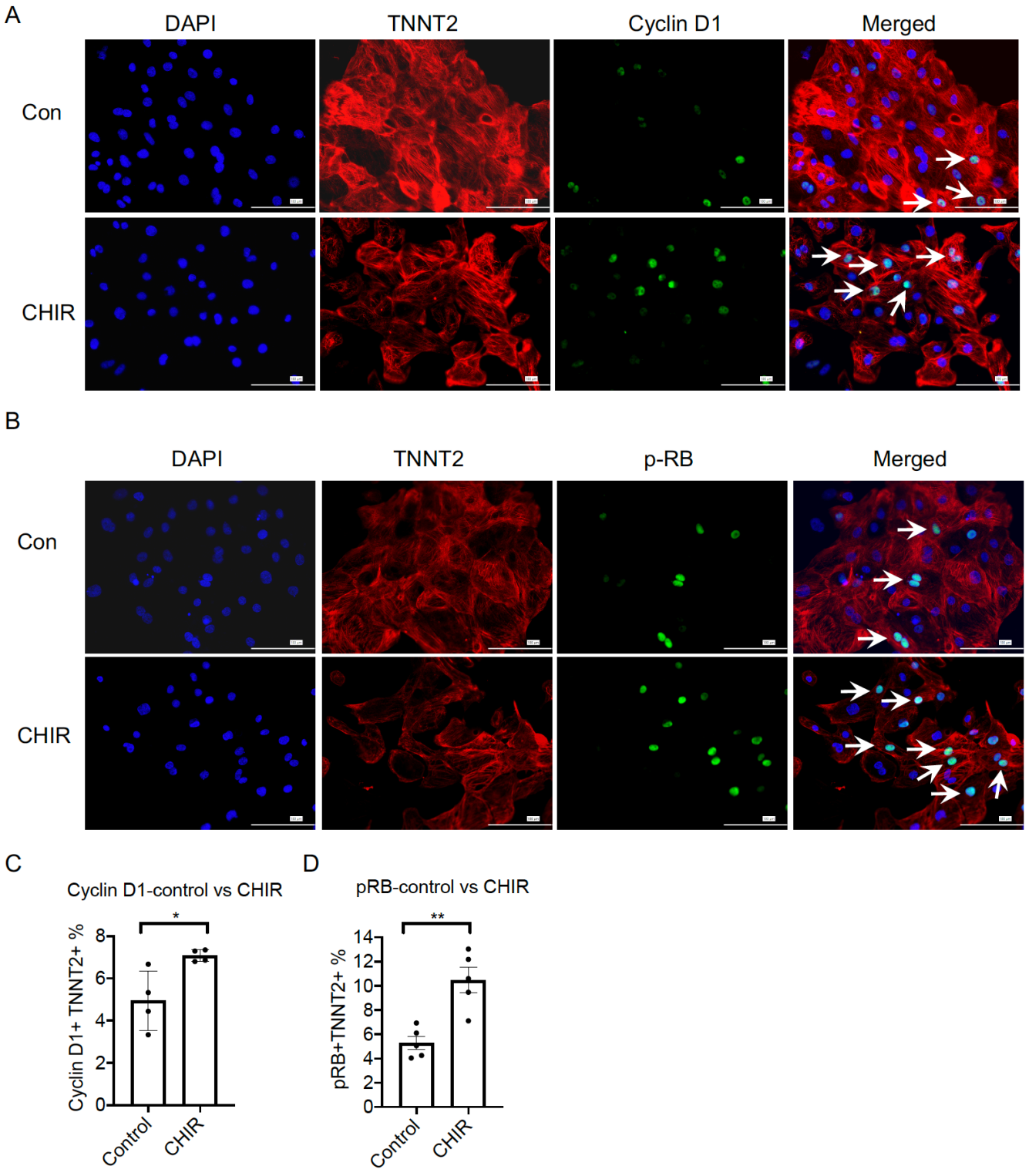

Figure S9. Cardiomyocyte proliferation identified by immunofluorescence staining with antibodies against Cyclin D1 and pRB. (**A**) Immunofluorescence staining using antibodies against TNNT2 (red) and Cyclin D1 (green). Nuclei are stained with DAPI (blue). (**B**) Immunofluorescence staining using antibodies against TNNT2 (red) and pRB (green) to identify proliferating cardiomyocytes. Nuclei are stained with DAPI (blue). (**C-D**) Quantitative analysis of percentages of proliferating cardiomyocytes identified by TNNT2+Cyclin D1+ (t-test, n=4) and TNNT2+pRB+ (t-test, n=5). Arrows indicate dividing iPSC-CMs. Data are presented as mean ± SEM. *p<0.05, **p<0.01. Scale bars: 100 μm.

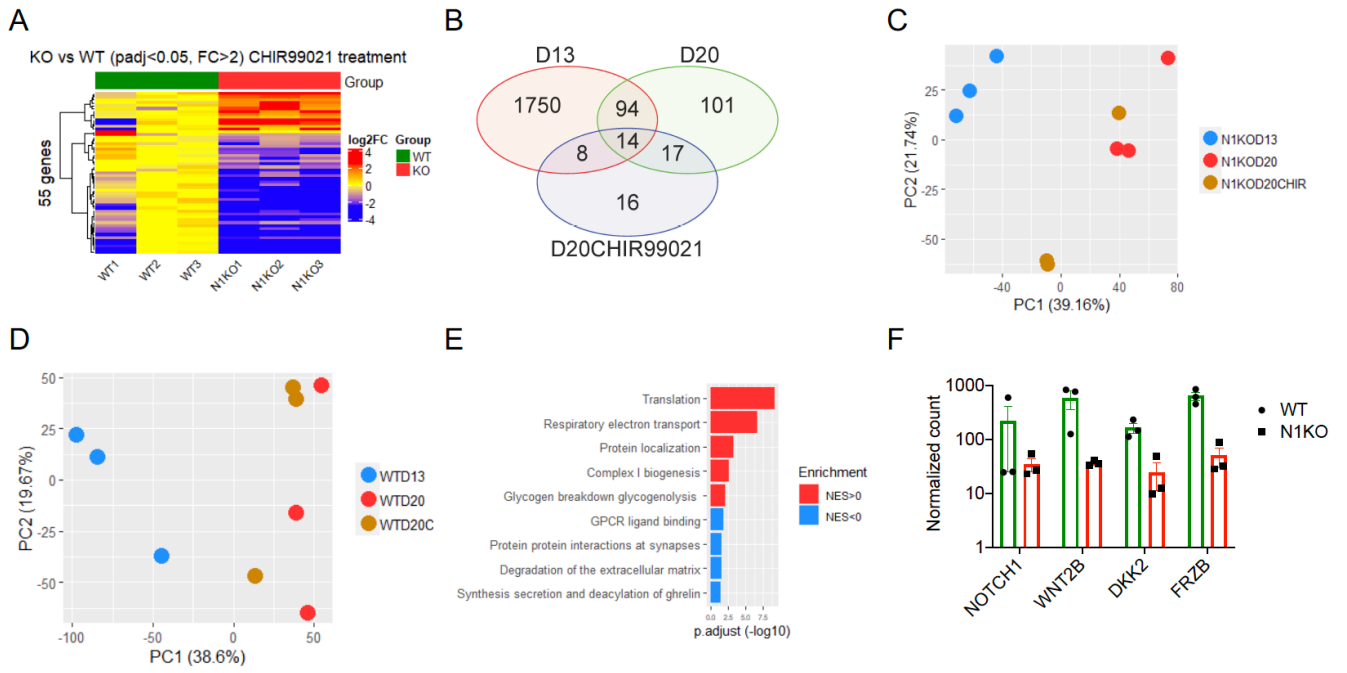

Figure S10. Transcriptional profiling of WT and N1KO iPSC-CMs in response to CHIR99021 treatment. (**A**) Heatmap illustration of DEGs between WT and N1KO iPSC-CMs in the presence of CHIR99021 (FDR < 0.05, fold change > 2). (**B**) Venn diagram of overlapped differentially expressed genes between WT and N1KO iPSC-CMs at D13 and D20 with and without CHIR99021. (**C-D**) PCA plot of all genes shows transcriptional shifts in the presence of CHIR99021 in both WT and N1KO iPSC-CMs at D13 and D20. (**E**) GSEA analysis shows upregulated and downregulated pathways that are associated with DEGs between WT and N1KO D20 iPSC-CMs with CHIR99021. (**F**) Expression levels of *NOTCH1, WNT2B, DKK2*, and FRZB are significantly decreased in N1KO compared to WT D20 iPSC-CMs (q-value < 0.01, n=3). Normalized counts are log10 transformed and median values of WT samples are used for baseline transformation for each gene. Data are presented as mean ± SEM.

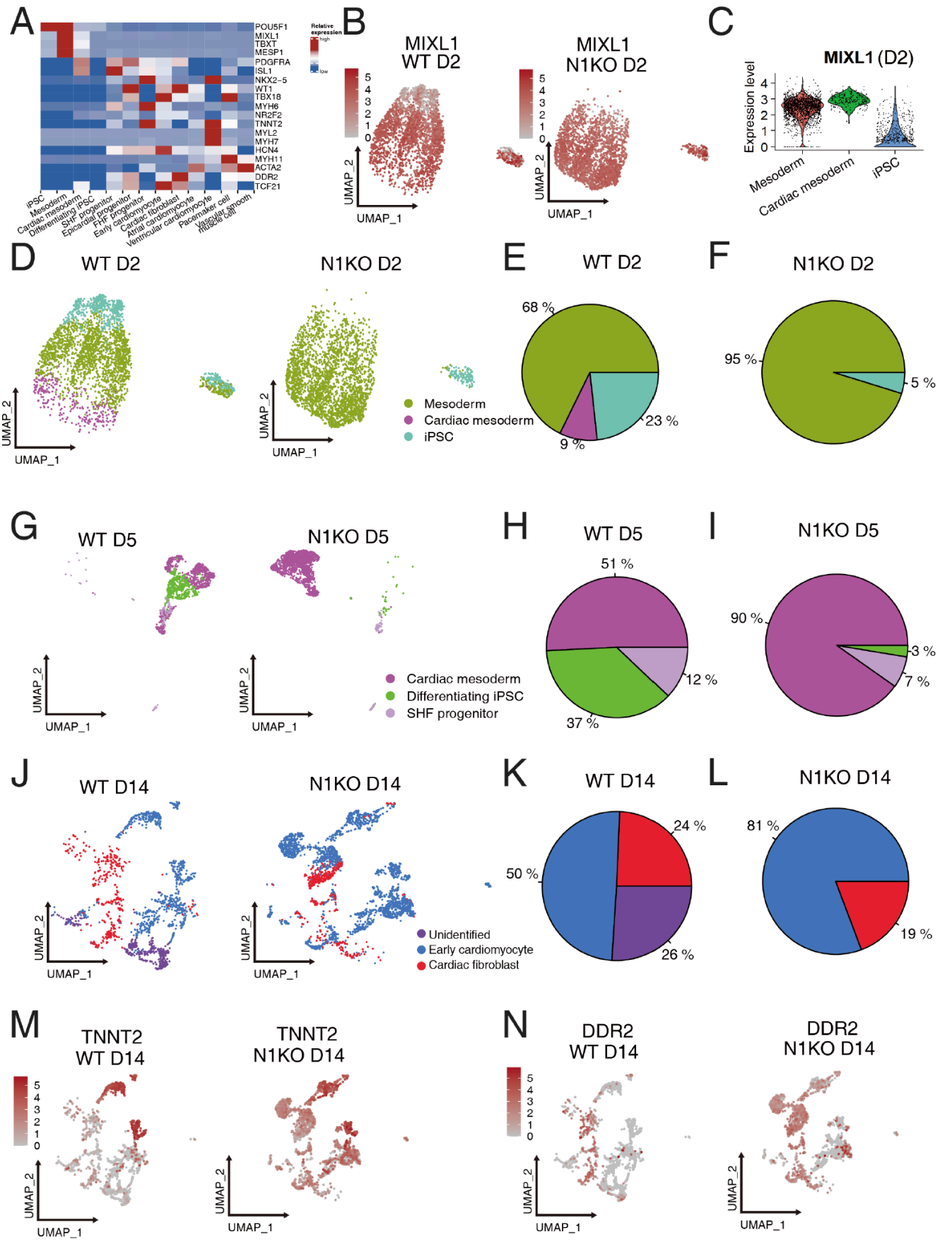
A
POU5F1
MIXL1
TBXT
MESP1
PDGFRA
ISL1
NKX2-5
WT1
TBX18
MYH6
NR2F2
TNNT2
MYL2
MYH7
HCN4
MYH11
ACTA2
DDR2
TCF21
iPSC
Mesoderm
Cardiac mesoderm
Differentiating iPSC
SHF progenitor
Epicardial progenitor
FHF progenitor
Early cardiomyocyte
Cardiac fibroblast
Atrial cardiomyocyte
Ventricular cardiomyocyte
Pacemaker cell
Vascular smooth muscle cell
B
MIXL1 WT D2
MIXL1 N1KO D2
UMAP_1
UMAP_2
C
MIXL1 (D2)
Expression level
Mesoderm
Cardiac mesoderm
iPSC
D
WT D2
N1KO D2
Mesoderm
Cardiac mesoderm
iPSC
E
WT D2
68 %
23 %
9 %
F
N1KO D2
95 %
5 %
G
WT D5
N1KO D5
Cardiac mesoderm
Differentiating iPSC
SHF progenitor
H
WT D5
51 %
12 %
37 %
I
N1KO D5
90 %
3 %
7 %
J
WT D14
N1KO D14
Unidentified
Early cardiomyocyte
Cardiac fibroblast
K
WT D14
24 %
50 %
26 %
L
N1KO D14
81 %
19 %
M
TNNT2 WT D14
TNNT2 N1KO D14
N
DDR2 WT D14
DDR2 N1KO D14

Figure S11. Single-cell transcriptomics shows the cell lineage composition and gene expression during cardiac differentiation of WT and N1KO iPSCs. (**A**) Cell type-specific marker gene expression in individual cell populations. (**B**) UMAP plotting of *MIXL1* expression in D2 WT and N1KO differentiating cells. (**C**) Violin plot shows the expression levels of *MIXL1* in mesoderm, cardiac mesoderm, and iPSC. (**D**) UMAP plotting of D2 WT and N1KO differentiating cells that include iPSC, mesoderm, and cardiac mesoderm. (**E-F**) Pie charts show percentages of individual cell populations in WT (E) and N1KO (F) D2 cells. (**G**) UMAP plotting of D5 WT and N1KO differentiating cells comprised of differentiating iPSC, cardiac mesoderm, and SHF progenitor. (**H-I**) Pie chart view of percentages of individual cell populations in WT (H) and N1KO (I) D5 cells. (**J**) UMAP plotting of D14 WT and N1KO cell populations containing early cardiomyocytes and cardiac fibroblasts (CFs). (**K-L**). Percentages of individual cell populations in WT (K) and N1KO (L) D14 cells. (**M-N**) UMAP plot shows the expression of cardiomyocyte-specific marker *TNNT2* (M) and fibroblast-specific marker *DDR2* (N) in D14 WT and N1KO cells.

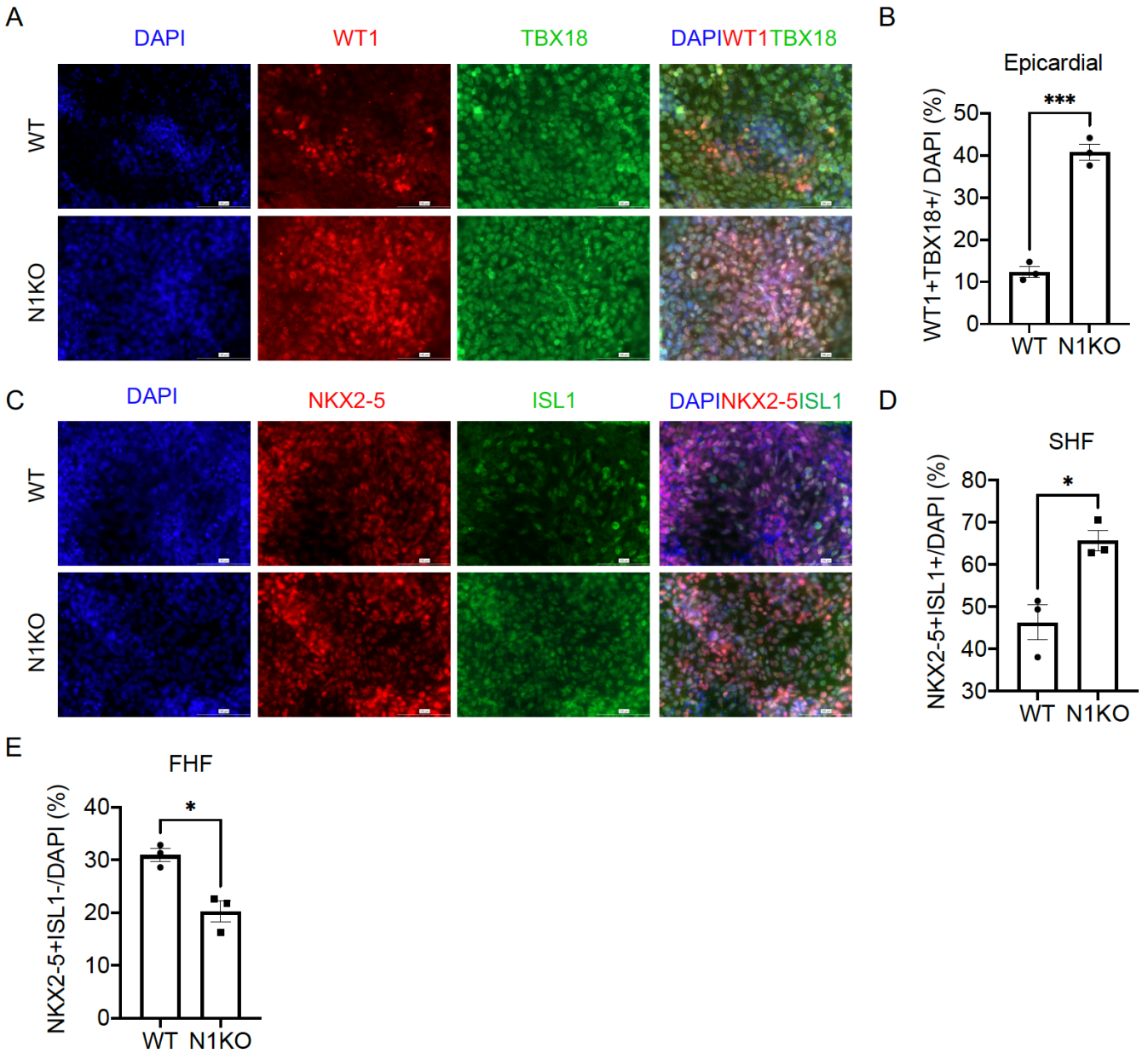

Figure S12. Functional validation of biased differentiation of cardiac progenitors (FHF, SHF, epicardial) in N1KO cells by immunofluorescence staining. (**A**) Identification of epicardial progenitors by co-expression of WT1 and TBX18 at D10 of differentiation. (**B**) Quantitation of the percentage of WT1+TBX18+ epicardial progenitors in both WT and N1KO. (**C**) Immunofluorescence staining of NKX2-5 and ISL1 to distinguish FHF and SHF progenitors at D10 of cardiac differentiation. (**D-E**) Quantitative analysis of the percentage of SHF (NKX2-5+ISL1+) (D) and FHF (NKX2-5+ISL1-) (E) progenitors in D10 N1KO and WT cells. Data are presented as mean ± SEM. *p<0.05, ***p<0.01, t-test, n=3 for each group. Scale bars: 100 μm.

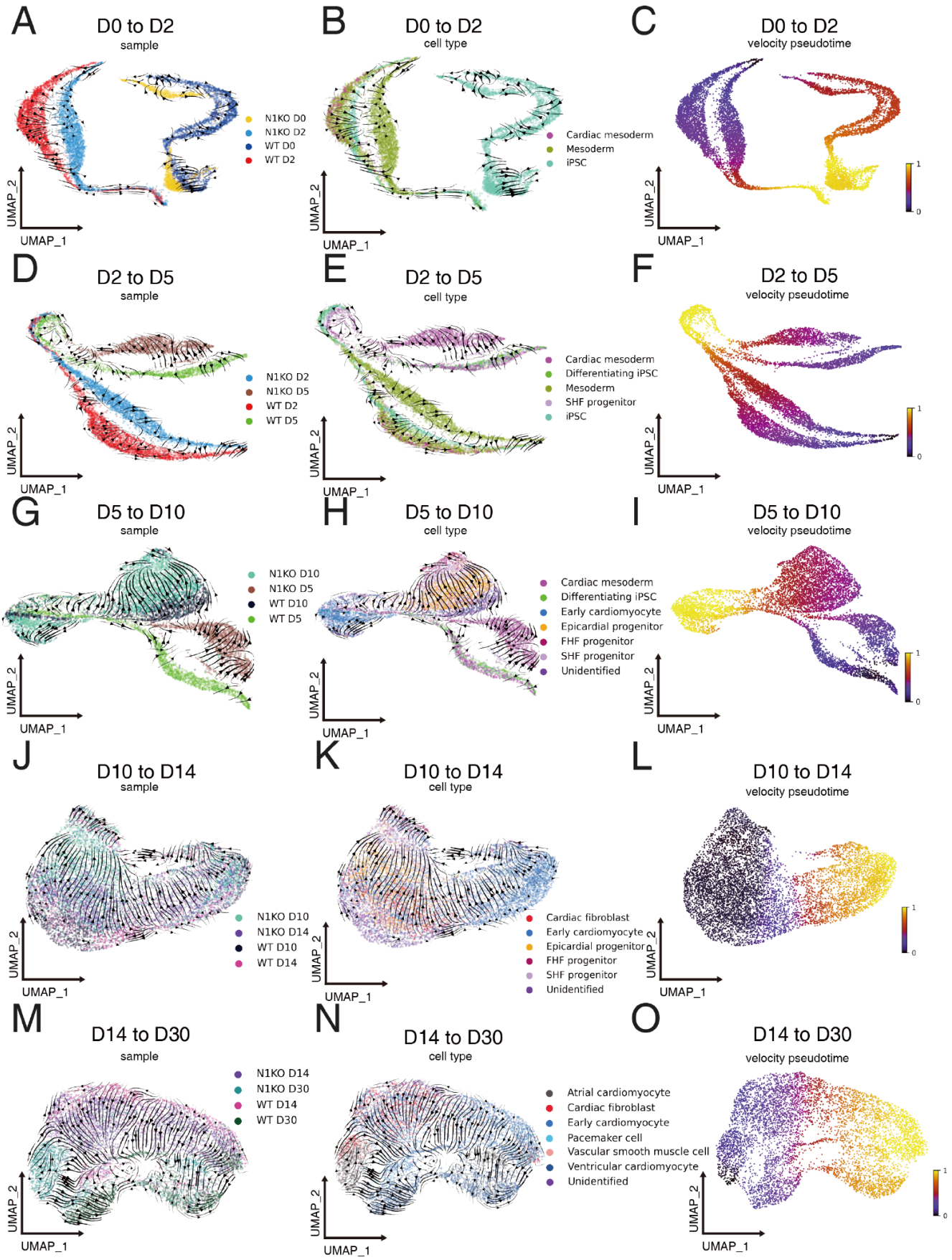
A
D0 to D2
sample
N1KO D0
N1KO D2
WT D0
WT D2
UMAP_2
UMAP_1
B
D0 to D2
cell type
Cardiac mesoderm
Mesoderm
iPSC
C
D0 to D2
velocity pseudotime
D
D2 to D5
sample
N1KO D2
N1KO D5
WT D2
WT D5
E
D2 to D5
cell type
Cardiac mesoderm
Differentiating iPSC
Mesoderm
SHF progenitor
iPSC
F
D2 to D5
velocity pseudotime
G
D5 to D10
sample
N1KO D10
N1KO D5
WT D10
WT D5
H
D5 to D10
cell type
Cardiac mesoderm
Differentiating iPSC
Early cardiomyocyte
Epicardial progenitor
FHF progenitor
SHF progenitor
Unidentified
I
D5 to D10
velocity pseudotime
J
D10 to D14
sample
N1KO D10
N1KO D14
WT D10
WT D14
K
D10 to D14
cell type
Cardiac fibroblast
Early cardiomyocyte
Epicardial progenitor
FHF progenitor
SHF progenitor
Unidentified
L
D10 to D14
velocity pseudotime
M
D14 to D30
sample
N1KO D14
N1KO D30
WT D14
WT D30
N
D14 to D30
cell type
Atrial cardiomyocyte
Cardiac fibroblast
Early cardiomyocyte
Pacemaker cell
Vascular smooth muscle cell
Ventricular cardiomyocyte
Unidentified
O
D14 to D30
velocity pseudotime

Figure S13. **Developmental trajectories inferred by RNA velocity during cardiac differentiation of WT and N1KO iPSCs. (A-C)** UMAP plotting of developmental trajectories from iPSC to mesoderm (D0 to D2) predicted by RNA velocity and clustered by samples (A), cell types (B), and pseudotime (C). (**D-F**) Predicted developmental trajectories from mesoderm (D2) to cardiac mesoderm (D5) are clustered by samples (D), cell types (E), and pseudotime (F). (**G-I**) Developmental routes from cardiac mesoderm (D5) to cardiac progenitors (D10) are indicated by samples (G), cell types (H), and pseudotime (I). (**J-L**) Converged developmental trajectories from cardiac progenitors (D10) to early cardiomyocytes (D14) between N1KO and WT cells are depicted by samples (J), cell types (K), and pseudotime (L). (**M-O**) Divergent developmental routes from early cardiomyocytes (D14) to fetal cardiomyocytes (D30) between N1KO and WT cells are illustrated by samples (M), cell types (N), and pseudotime (O).

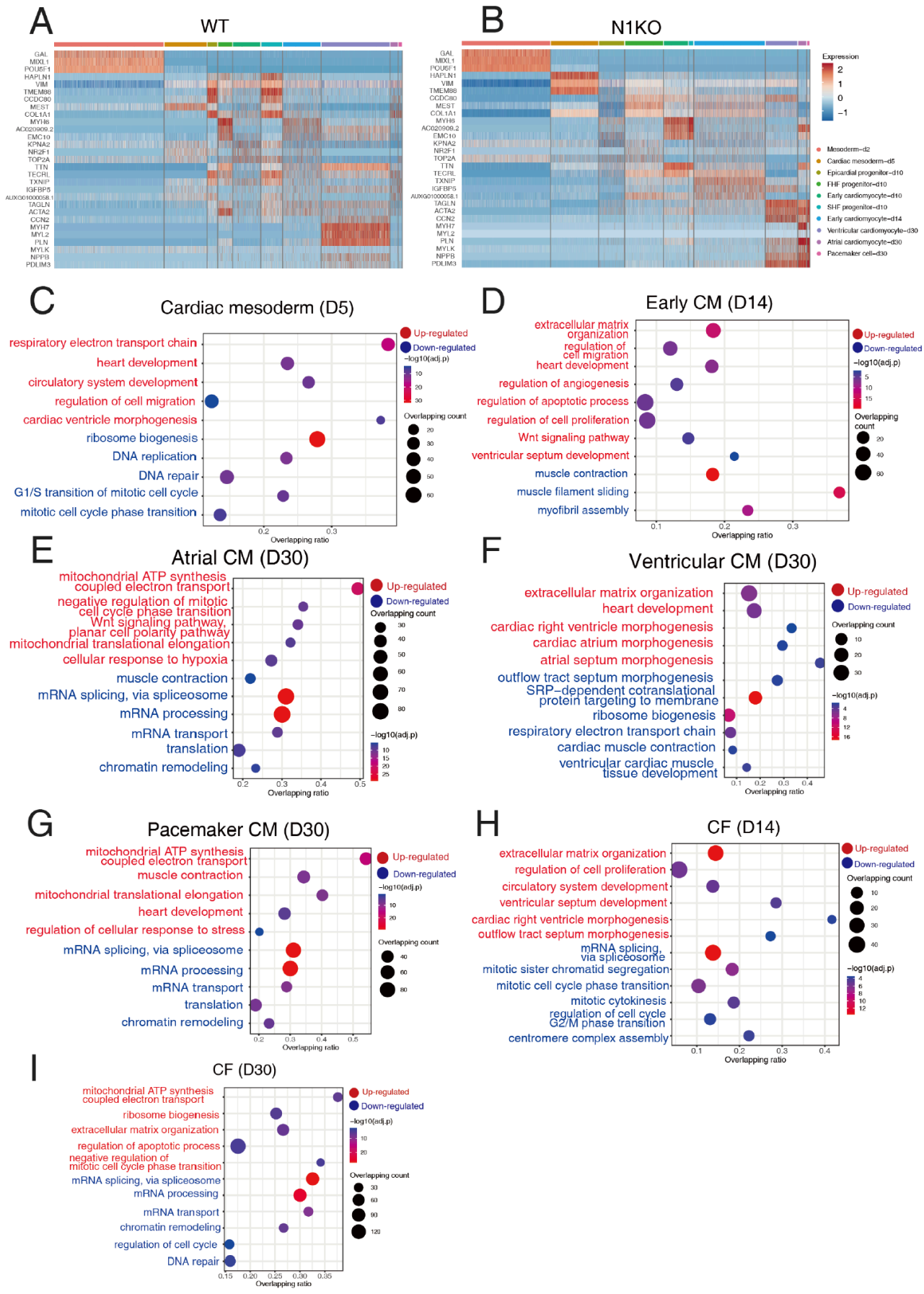
A
WT
B
N1KO
GAL
MIXL1
POU5F1
HAPLN1
VIM
TMEM88
CCDC80
MEST
COL1A1
MYH6
AC020909.2
EMC10
KPNA2
NR2F1
TOP2A
TTN
TECRL
TXNIP
IGFBP5
AUXG01000058.1
TAGLN
ACTA2
CCN2
MYH7
MYL2
PLN
MYLK
NPPB
PDLIM3
Expression
2
1
0
−1
Mesoderm−d2
Cardiac mesoderm−d5
Epicardial progenitor−d10
FHF progenitor−d10
Early cardiomyocyte−d10
SHF progenitor−d10
Early cardiomyocyte−d14
Ventricular cardiomyocyte−d30
Atrial cardiomyocyte−d30
Pacemaker cell−d30
C
Cardiac mesoderm (D5)
respiratory electron transport chain
heart development
circulatory system development
regulation of cell migration
cardiac ventricle morphogenesis
ribosome biogenesis
DNA replication
DNA repair
G1/S transition of mitotic cell cycle
mitotic cell cycle phase transition
Up-regulated
Down-regulated
−log10(adj.p)
Overlapping count
Overlapping ratio
D
Early CM (D14)
extracellular matrix organization
regulation of cell migration
heart development
regulation of angiogenesis
regulation of apoptotic process
regulation of cell proliferation
Wnt signaling pathway
ventricular septum development
muscle contraction
muscle filament sliding
myofibril assembly
E
Atrial CM (D30)
mitochondrial ATP synthesis coupled electron transport
negative regulation of mitotic cell cycle phase transition
Wnt signaling pathway, planar cell polarity pathway
mitochondrial translational elongation
cellular response to hypoxia
muscle contraction
mRNA splicing, via spliceosome
mRNA processing
mRNA transport
translation
chromatin remodeling
F
Ventricular CM (D30)
extracellular matrix organization
heart development
cardiac right ventricle morphogenesis
cardiac atrium morphogenesis
atrial septum morphogenesis
outflow tract septum morphogenesis
SRP−dependent cotranslational protein targeting to membrane
ribosome biogenesis
respiratory electron transport chain
cardiac muscle contraction
ventricular cardiac muscle tissue development
G
Pacemaker CM (D30)
mitochondrial ATP synthesis coupled electron transport
muscle contraction
mitochondrial translational elongation
heart development
regulation of cellular response to stress
mRNA splicing, via spliceosome
mRNA processing
mRNA transport
translation
chromatin remodeling
H
CF (D14)
extracellular matrix organization
regulation of cell proliferation
circulatory system development
ventricular septum development
cardiac right ventricle morphogenesis
outflow tract septum morphogenesis
mRNA splicing, via spliceosome
mitotic sister chromatid segregation
mitotic cell cycle phase transition
mitotic cytokinesis
regulation of cell cycle G2/M phase transition
centromere complex assembly
I
CF (D30)
mitochondrial ATP synthesis coupled electron transport
ribosome biogenesis
extracellular matrix organization
regulation of apoptotic process
negative regulation of mitotic cell cycle phase transition
mRNA splicing, via spliceosome
mRNA processing
mRNA transport
chromatin remodeling
regulation of cell cycle
DNA repair

Figure S14. *NOTCH1* deficiency leads to differential gene expression profiles in cardiac mesoderm, early cardiomyocytes, fetal cardiomyocytes and cardiac fibroblasts. (**A-B**) Top 3 enriched genes in individual cell types in WT (A) and N1KO (B) cells across developmental stages. (**C**) Upregulated and downregulated pathways that are enriched in D5 cardiac mesoderm in N1KO versus WT samples. (**D**) Upregulated and downregulated pathways that are enriched in D14 early cardiomyocytes in N1KO versus WT samples. (**E-G**) Upregulated and downregulated pathways that are associated with DEGs in D30 atrial-like cardiomyocytes (E), ventricular-like cardiomyocytes (F), and pacemaker-like cells (G) in N1KO compared to WT samples. (**H-I**) Upregulated and downregulated pathways that are enriched in D14 (H) and D30 (I) cardiac fibroblasts in N1KO versus WT samples. Top enriched pathways are selected based on q-value <0.01. The X-axis shows the ratio of enriched pathways versus background. The Y-axis represents the term of enriched pathways that are upregulated (in red) or downregulated (in blue). The sizes of the dots indicate the number of target genes in a given pathway whereas the colors of the dots reflect log-transformed adjusted p-values.

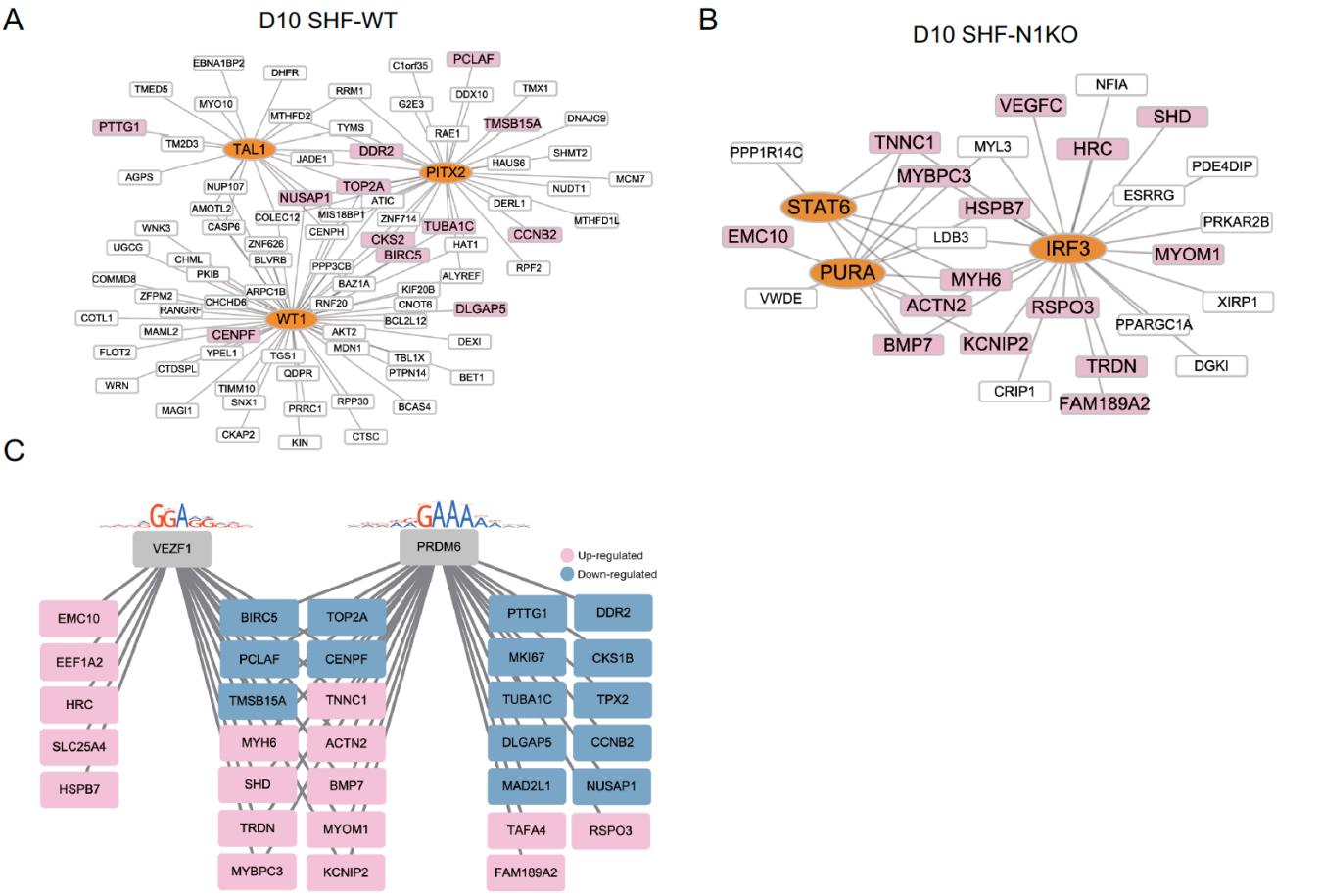

Figure S15. Altered gene regulatory networks (GRNs) in D10 cardiac progenitor cells due to *NOTCH1* deficiency. (**A-B**) Visualization of top 3 TFs in WT (A) and N1KO (B) D10 SHF progenitors. TFs are ranked by regulon specificity scores using the IRIS3 web server and highlighted in orange in the ellipse shape. Differentially expressed genes between WT and N1KO are highlighted in pink. (**C**) Common TFs (VEZF1 and PRDM6) were inferred in both WT and N1KO D10 SHF progenitors. Shared DEGs that are prospectively regulated by both VEZF1 and PRDM6 are shown in the middle columns.

Table S1. Single guide RNA (sgRNA) sequences for deletion of *NOTCH1* in human iPSCs

Name	Sequences
sgRNA-NOTCH1_5	Forward 5’ CACCGTCGGGACGCGCGGCTCAGCT 3’ Reverse 5’ AAACAGCTGAGCCGCGCGTCCCGAC 3’
sgRNA-NOTCH1_7	Forward 5’ CACCGGACTCCCACTTAGTGACCC 3’ Reverse 5’ AAACGGGTCACTAAGTGGGAGTCC 3’

Table S2. Outside and inside screening primers for genotyping *NOTCH1* KO iPSC clones.

Name	Sequences	Length of PCR products
Outside primers	Forward 5' AATTTCAGTCGCCAGTTGTCGCCGA 3' Reverse 5' CAGAGGAGGCATCACTACCAGC 3'	2,829bp for WT, 409bp for homozygous KO.
Inside primers	Forward 5' AATTTCAGTCGCCAGTTGTCGCCGA 3' Reverse 5' CAGAGGAGGCATCACTACCAGC 3'	699 bp for WT, no band for homozygous KO.

Table S3. TaqMan gene expression assays.

Category	Gene Symbols	TaqMan Assays
Ligand	*DLL4*	Hs00184092_m1
NOTCH receptor	*NOTCH1*	Hs01062014_m1
	NOTCH4	Hs00965889_m1
NOTCH target	*HEY1*	Hs01114113_m1
	HEY2	Hs01012057_m1
Arterial EC marker	*EFNB2*	Hs00187950_m1
Venous EC marker	*NR2F2*	Hs00819630_m1
	EPHB4	Hs01119113_m1

Table S4. Lineage-specific genes used for annotating cell populations in scRNA-seq data analysis.

Cell lineages	Markers
Pluripotent stem cells (iPSCs)	POU5F1+ NANOG+
Mesoderm	TBXT+ MIXL1+
Cardiac mesoderm	MESP1+ PDGFRA+
SHF progenitors	NKX2-5+ ISL1+
FHF progenitors	NKX2-5+ ISL1-
Epicardial progenitors	WT1+ TBX18+
Atrial cardiomyocytes	NR2F2+ MYH6+ TNNT2+
Ventricular cardiomyocytes	MYL2+ MYH7+ TNNT2+
Pacemaker cells	HCN4+ TNNT2+
Vascular endothelial cells	PECAM1+ CDH5+
Vascular smooth muscle cells	MYH11+ ACTA2+
Cardiac fibroblasts	DDR2+ TCF21+